Influence of Thermocapillary Convection on Solid-liquid Interface

K. Matsunaga[1] and H. Kawamura[1]

Abstract: Existing studies on solidification phenomena mainly focused on the solidification processes per se. In real systems, however, one cannot neglect the effects of molten material convective flow, such as natural and thermocapillary convection (they strongly affect the resulting quality of the solidified materials). The present study aims to experimentally investigate on the effect of the thermocapillary flow upon the directional solidification in a liquid layer with a free upper surface. If no free surface exists, the solid–liquid interface (SLI) is vertical and straight, while, with the free surface, the SLI is inclined against the wall-normal direction and is curved in the growth direction due to thermocapillary convection. The dendrite tip, which is parabolic in a stagnant liquid, is deformed asymmetrically due to surface flow. The secondary dendrite arm is larger in the inflow direction of convection. It is also found that even if the growth rate of the SLI near the top and bottom surface is the same at equilibrium, there exists a distinct difference in the solidification morphology.

keyword: Solidification, Free surface, Thermocapillary convection, Solid-liquid interface, Morphology, Liquid layer.

1 Introduction

The demand for single crystals of high quality is increasing rapidly. It is well known that the quality of crystals is affected by growth parameters and conditions. For instance, non axisymmetric isotherms lead to a solid-liquid interface (SLI) non-normal to the seeding axis. These non axisymmetric isotherms can be induced by factors such as convective instability and temperature fluctuations. Convection in the melt has a significant impact on the quality of the crystal. It affects both thermal and dopant distributions (several researches have already conducted on this subject). For instance, Esaka, Taenaka, Ohishi, Mizoguchi and Kajioka (1989) have studied the

growth of dendrites in forced flow.

The space is expected to be an ideal environment to process high-quality materials or crystals because buoyant forces are almost negligible. However, thermocapillary convection takes place inevitably even in the space environment. The thermocapillary-driven convection arises if a non-uniform temperature distribution exists over a free surface. Thus, flow induced by the thermocapillary force and its effect upon the crystal growth must be investigated.

It should be noted here that most of past researches focused on either crystal growth or thermocapillary convection as disjoint subjects (see, e.g., Lappa, 2005a, 2005b; Lan and Yeh, 2005; Gelfgat et al., 2005; Tsukada et al., 2005). Recently Wei and Ming (1991) and Schwabe, Xiaodong and Scharmann (1996) have reported that a shape of the SLI is significantly affected by thermocapillary convection (see also Amberg and Shiomi, 2005). Baskar and Nicholas (2004) examined numerically the influence of a magnetic field gradient on the directional solidification with thermocapillary convection in a liquid layer. Along these lines, the present study aims to investigate experimentally the effect of the thermocapillary convection upon the directional solidification in a liquid layer with a free surface.

2 Experiment

In this experiment, succinonitrile-acetone (SCN-ACE) system is used as test fluid. This is often used for solidification experiments, because the coagulation form of this material is similar to a real metal and its physical properties and phase diagram are known in detail. Table 1 shows physical properties of the SCN. The purchased purity of the SCN was 98 % and its freezing point was 58.08 ^{o}C. It was distilled four times under vacuum before the experiment. The mass concentration of the acetone was either 0.3 % or 1.3 %. Experimental setup is shown in Fig. 1. Basically this set-up is a typical Bridgman-type furnace and one can control independently the temperature gradient and the growth velocity.

[1] Dept. Mech. Eng., Faculty of Sci. & Tech., Tokyo University of Science, Tokyo, Japan
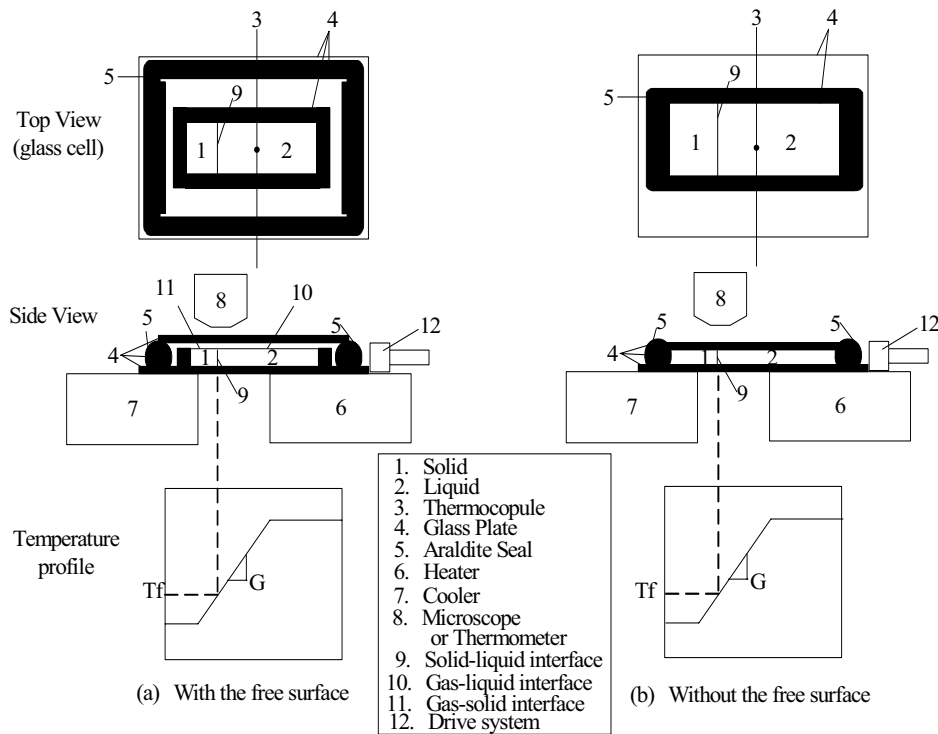
Figure 1 : Illustration of the experimental arrangement.

Two types of glass cells were prepared. In type (a), a thin Ar gas layer was introduced between the liquid layer and the top glass cover plate to realize a gas-liquid interface. In type (b), Ar gas layer was eliminated and the liquid layer contacted directly to the top glass cover plate. The test fluid volume was $40 \times 20 \times 0.7$ mm^3. A thermocouple of 0.05 mm was placed into the glass cells. The thermocouple had little effect on the structures because it was placed parallel to the isotherms, and its diameter was much smaller than the cell gap. A constant temperature profile was established in the glass cell by employing a heater and a cooler.

In the following section, we describe two types of experiment. In section (1), the glass cell is stationary and the SLI is in equilibrium. In section (2), the glass cell is moved by a motor with feedback control so that the SLI grows and a steady state growth is obtained.

3   Results and discussion

3.1   Stationary SLI

Figure 2 shows shapes of the SLI (a) with and (b) without free surface. The temperature gradient is 58 K/cm, and observation areas are near the center of the test fluid

Table 1 : Physical properties of SCN-ACE.

C_0 (wt%)	0.3	1.3
T_L (^{o}C)	57.2	54.2
ΔT_0 (K)	7.58	32.8
D (m^2/sec)	-	1.3×10^{-9}
k (-)	0.18	0.1
m (K/wt%)	-	-2.8
T_f (^{o}C)	58.08	
ρ (kg/m^3)	0.988×10^3	
μ (kg/ms)	2.54×10^{-3}	
κ (m^2/sec)	1.16×10^{-7}	
σ_T (N/mK)	1.06×10^{-4}	

volume. With the free surface, a span wise curvature is observed in the SLI. In Fig. 2 (a), we can see two curved interface lines between solid and liquid phases. Left one is near the free surface and right one near the bottom plate. It indicates that the SLI is inclined in the direction of thickness.

The illustration of these shapes of the SLI with possible thermocapillary flow fields is given in Fig. 3. Without the free surface, (Fig. 3 (b)), the SLI is straight and
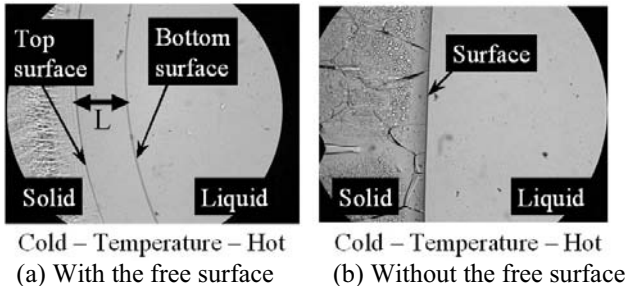
Figure 2 : Top view of solid-liquid interface near the sidewall. View area = 4.3×3.2 mm². Temperature gradient = 58.0 K/cm. Ma=1024. Acetone concentration=1.3 wt%.
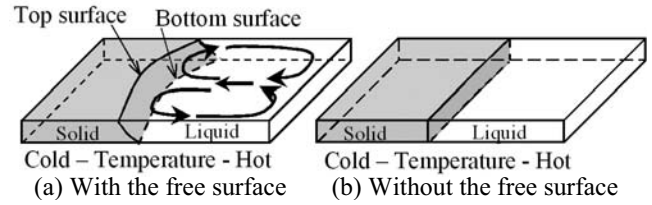

Figure 3 : Comparison of interface shape for "with" and "without" free surface.
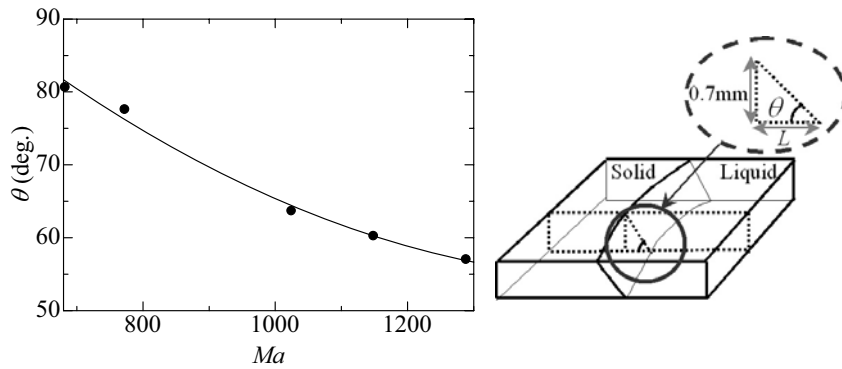

Figure 4 : Correlation between θ and Ma.

vertical against the cover and base plates. On the other hand, with the free surface, thermocapillary convection is induced from liquid towards the SLI over the free surface, because the SLI is colder than the bulk of the liquid. Since the liquid volume is limited span wisely by the side plates, the thermocapillary flow is strongest in the center. Thus a pair of recirculating flows as shown in Fig. 3 (a) occurs over the free surface. This is the reason why the interface line is curved in Fig. 2 (a) and Fig. 3 (a). Since the surface thermocapillary flow carries hot liquid from the hot side of the cell, accordingly, the upper part of the SLI is hotter than the lower one. This causes the inclination of the SLI as seen in Fig. 2 (a) and Fig. 3 (a). This is in accordance with the finding by Baskar and Nicholas (2004) through their numerical simulation. Figure 4 shows the inclination angle θ (see Fig. 4) as a function of the Marangoni number *Ma* defined as $\sigma_T G d^2/\mu\kappa$, where σ_T: surface tension of coefficient, *G*: Temperature gradient $=|\Delta T/\Delta x|$, *d*: thickness of test area, μ: viscosity, κ: liquid heat transfer coefficient. The temperature difference between the heater and

the cooler is defined by ΔT. The gap of the heater and the cooler Δx is 25 mm. The angle θ gradually decreases as *Ma* is increased. In addition, to measure the temperature field, a radiation thermometer was employed. The obtained thermal contour with the free surface is shown in Fig. 5. An isotherm interval is 5 K. The arrow shows the position of the SLI. In the bulk liquid, the isotherms curved along the SLI. Consequently, the significant variation in the curvature of the SLI can be attributed mainly to the strong convection in the liquid.

3.2 Growing SLI

A servomotor was employed to drive the glass cell from a heating to a cooling condition as shown in Fig. 1. It has been observed that the morphology of the SLI becomes planar, cellular and dendrite.

3.2.1 Dendritic growth

Dendrites are the most common microstructure growing naturally during solidification of alloys and pure metals. Figure 6 shows a dendritic SLI, which grow from left to
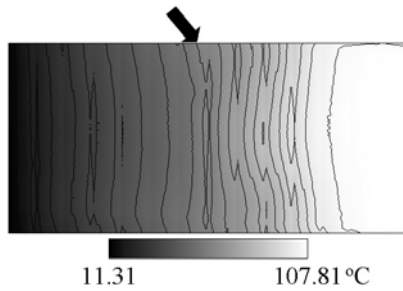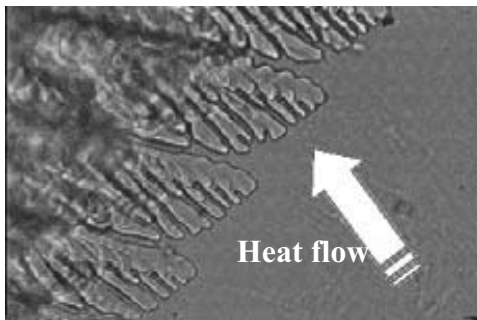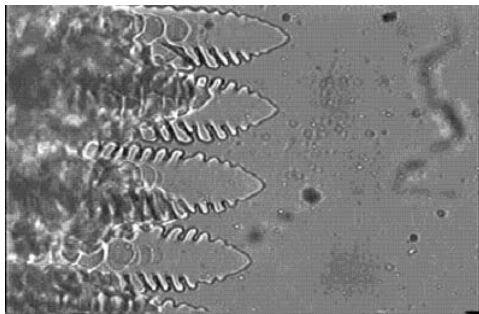
Figure 5 : Top view of the temperature of isotherm. View area =15×7 mm². Temperature gradient =38.0 K/cm. Ma=678. Black arrow shows the position of solid-liquid interface.

(a) With the free surface (Thermocapillary convection) Temperature gradient =43.0 K/cm.

(b) Without the free surface. Temperature gradient =60.0 K/cm.

Figure 6 : Dendrite growth with and without free surface. View area=0.82×0.61 mm². Growth velocity= 20 μm/sec. Acetone concentration =1.3 wt%.

right (a) with and (b) without free surface. Without the free surface, the secondary dendrite arms grow symmetrically against a dendrite trunk. (see Fig. 6 (b)) On the other hand, with the free surface, they grow asymmetrically against the dendrite trunk. (see Fig. 6 (a)). It is known that the secondary dendrite arms grow along the direction of heat flow if the temperature gradient is large.

Since thermocapillary convection causes the inclination of the isotherm as previously discussed, as a result, the secondary dendrite arms tend to grow in the upstream direction of the heat flow, which is normal to the isotherm.

3.2.2 Solidification morphology

It is known that if effects of convective flow upon the molten material are neglected, the SLI morphology mainly depends on the temperature gradient and the growth rate of the SLI. Tiller, Jackson, Rutter and Chalmers (1953) estimated the growth rate V_c at which a planar SLI breaks under the condition of constitutional undercooling. It can be expressed as

$$V_c = \frac{GD}{\Delta T_0}, \tag{1}$$

where G is the temperature gradient at the SLI, ΔT_0 the liquidus-solidus temperature range at the initial alloy concentration and D the diffusion coefficient in the liquid.

Kurz and Fisher (1981) obtained the growth rate for the cell-to-dendrite transition (for $k < 1$) as

$$V_{tr} = \frac{GD}{k\Delta T_0}, \tag{2}$$

where k is the equilibrium distribution coefficient. These transition velocities varying with G can be calculated using the physical properties of the succinonitrile-acetone system given in table 1. The distribution map of the SLI morphology for SCN-0.3 wt% ACE alloy will be presented later using Eqs. (1) and (2).

Figures 7 (a) and (b) show the SLI at the growth velocity of 24 μm/sec with free surface. Figure 7 (a) focuses on the bottom surface of the SLI indicating that the SLI morphology is dendrite. On the other hand, Fig. 7 (b) focuses on the top surface indicating a cellular morphology. Accordingly there exists a distinct difference in the solidification morphology between the top and the bottom surface. The coexistence of the solidification morphology has never been observed in systems without the free surface. We traversed the focused plane from cellular (top) to the dendrite (bottom) structures and no SLI was found between them. This indicates that a side view of this coexisting morphology could be depicted as shown in Fig. 8.

Figure 9 shows the comparison of the solidification morphology at the bottom surface according to the present
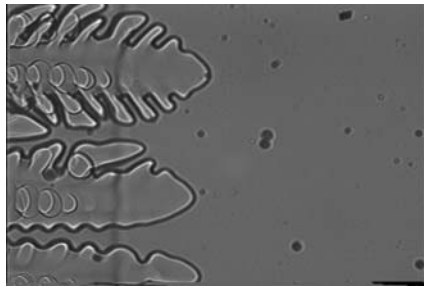
(a) SLI (focused on the bottom surface)
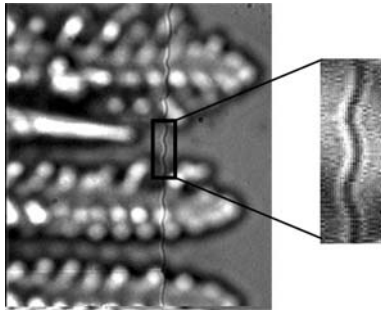
(b) SLI (focused on the top surface)

Figure 7 : Difference of morphology between top and bottom surfaces in SCN-1.3 wt% ACE. View area = 0.82×0.61 mm^2. Temperature gradient =24.0 K/cm.
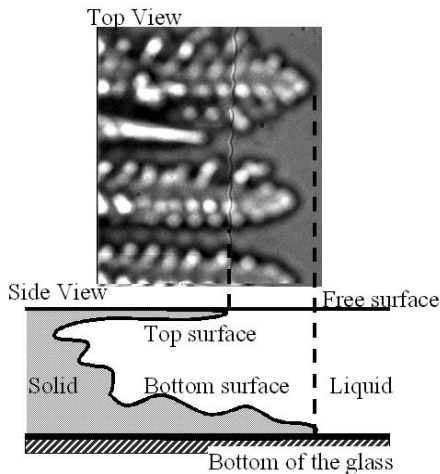

Figure 8 : Conceptual sketch of the SLI.

Figure 9 : Distribution map of the solidification morphology at the bottom surface in SCN-0.3 wt % ACE.
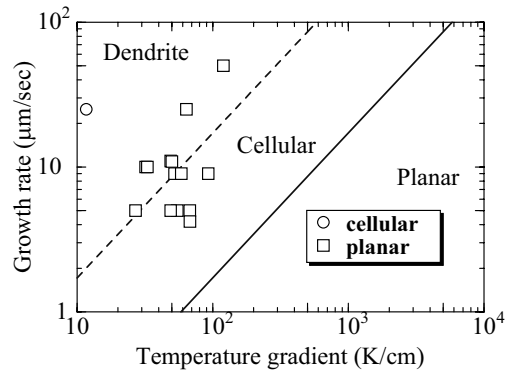
Figure 10 : Distribution map of the solidification morphology at the top surface in SCN-0.3 wt % ACE.

experimental results and theoretical ones (obtained with Eqs. (1) and (2)). The label "dendritic-cellular" means an intermediate structure in which dendritic disturbance develops but no secondary branch is yet observed. The temperature gradient G was calculated by the temperature at the bottom in the liquid and the traversing velocity of the glass cell. Although the thermocapillary convec-
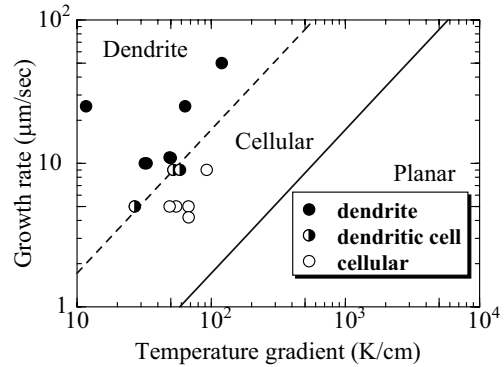
tion exists, the existing conditions of dendrite and cellular structures show a good agreement with the theoretical lines.

On the other hand, for the free surface, observed SLI morphology does not agree with the theories as shown in Fig. 10. Since the temperature of the top surface was not measured directly, the temperature gradient was assumed to be same as the bottom one in the plot of Fig. 10. In reality however, the temperature gradient near the SLI at the top surface might be greater than the bottom one. Because hotter fluid approaches to the SLI, where the temperature is kept at the solidification point. We find that the experimentally observed morphology at the top surface does not agree with the theories. This is probably because the actual temperature gradient at the top surface would be greater than the plotted one as discussed above and/or because the existence of surface kinetic energy suppressed the onset of dendritic structures. Further

experiments are necessary to investigate these effects on the SLI morphology.

4   Conclusions

The effect of thermocapillary convection upon the directional solidification in liquid layer with a free surface has been investigated experimentally. When equilibrium of the SLI is established, the SLI is inclined against the wall-normal direction and is curved in the growth direction due to the thermocapillary convection. When the SLI grows, the secondary dendrite arm is deformed asymmetrically due to thermocapillary convection. The secondary dendrite arm is larger in the inflow direction of the convection. It is also found that even if the growth rate of the SLI near the top and bottom surface is the same at equilibrium, there exists a distinct difference in the solidification morphology near these surfaces.

References

Amberg, G.; Shiomi, J. (2005) : Thermocapillary flow and phase change in some widespread materials processes. *Fluid Dyn. Mater. Process*, Vol. 1, pp. 81-95.

Baskar, G.; Nicholas, Z. (2004): Using magnetic field gradients to control the directional solidification of alloys and the growth of single crystals, *J. Crystal Growth*, vol. 270, pp.255-272.

Chopra, M-A. (1983): Influence of diffusion and convective transport on dendritic growth in dilute alloys, Rensselaer Polytechnic institute.

Esaka, H.; Kurz, W. (1985): Columnar dendrite growth: Experiments on tip growth, *J. Crystal Growth*, vol72, p.578-584.

Esaka, H.; Taenaka, T.; Ohishi, H.; Mizoguchi, S.; Kajioka, H. (1989): Deflection mechanism of columnar dendrite due to fluid flow, *JASMA*, vol. 6, pp. 20-25.

Gelfgat A.Yu., Rubinov A., Bar-Yoseph P.Z. and Solan A., (2005): On the Three-Dimensional Instability of Thermocapillary Convection in Arbitrarily Heated Floating Zones in Microgravity Environment , *Fluid Dyn. & Mater. Proc.*, Vol. 1, No.1, pp 21-32

Kurz, W.; Fisher, D-J. (1981): Dendrite growth at the limit of stability: Tip radius and spacing, *Acta Metallurgica*, vol.29, pp. 11-20.

Lan C. W., Yeh B.C., (2005): Effects of rotation on heat flow, segregation, and zone shape in a small-scale floating-zone silicon growth under axial and transversal magnetic fields, *Fluid Dyn. & Mater. Proc.*, Vol. 1, No. 1, pp. 33-44.

Lappa M., (2005a): On the nature and structure of possible three-dimensional steady flows in closed and open parallelepipedic and cubical containers under different heating conditions and driving forces, *Fluid Dyn. & Mater. Proc.*, Vol. 1 No. 1, pp. 1-19.

Lappa M., (2005b): Review: Possible strategies for the control and stabilization of Marangoni flow in laterally heated floating zones, *Fluid Dyn. & Mater. Proc.*, Vol. 1, No.2, pp. 171-188.

Ramagopal, A.; William, G. (1988) Dendritic Growth with Thermal Convection, *J. Crystal Growth*, vol.91, pp.587-598.

Schwabe, D.; Xiaodong, D.; Scharmann, A. (1996): Unstable flow and solidification speed due to the interaction of thermocapillary and solutocapillary forces in directional solidification, *J.Crystal Growth*, vol. 166, pp. 483-488.

Tiller, W-A.; Jackson, K-A.; Rutter, J-W.; Chalmers, B. (1953): The redistribution of solute atoms during the solidification of metals, *Acta Metallurgica*, vol.1, pp. 428-437.

Toenhardt, R.; Amberg, G. (2000): Simulation of natural convection effects on SCN crystals, *Physical Review E*, vol. 62, pp828-836.

Tsukada T., Kobayashi M., Jing C.J. and Imaishi N., (2005): Numerical simulation of CZ crystal growth of oxide, *Fluid Dyn. & Mater. Process*, Vol. 1, No.1, pp. 45-62.

Wei, S.; Ming, H-C. (1991): Interaction of thermocapillary and natural convection flows during solidification: normal and reduced gravity conditions, *J. Crystal Growth*, vol.108, pp.247-261.